Distribution of Disulfide Bonds in the Two-Disulfide Intermediates in the Regeneration of Bovine Pancreatic Ribonuclease A: Further Insights into the Folding Process†

Michael J. Volles,‡ Xiaobing Xu,§ and Harold A. Scheraga*

Baker Laboratory of Chemistry and Chemical Biology, Cornell University, Ithaca, New York 14853-1301

Received March 11, 1999; Revised Manuscript Received April 12, 1999

ABSTRACT: The distribution of one-disulfide bonds in the two-disulfide intermediates in the oxidative refolding of bovine pancreatic ribonuclease A has been characterized. These two-disulfide intermediates were formed from the fully reduced denatured protein by oxidation with dithiothreitol, then blocked with AEMTS, purified by cation-exchange chromatography, enzymatically digested, and analyzed by reversed-phase high-performance liquid chromatography and mass spectrometry. The relative concentration of each of the 28 possible one-disulfide bonds in the two-disulfide ensemble was determined. Comparison with a statistical mechanical treatment of loop formation shows that the two-disulfide intermediates are probably compact. All 28 disulfide bonds were observed, demonstrating the absence of specific long-range interactions in these intermediates. Thermodynamic arguments suggest that the absence of such specific long-range interactions in the two-disulfide species may elevate the concentration of kinetically important three-disulfide intermediates and thereby increase the folding rate. Bond [65−72] was found to make up ∼27% of the disulfide bonds of the two-disulfide species, significantly more than all other disulfides, because of stabilization by loop entropy factors and an energetically favorable β-turn. This turn may be one of several chain-folding initiation sites, accelerating folding by decreasing the dimensionality of the conformational space that has to be searched.

This paper is a continuation of our recent efforts to elucidate the interactions that determine the folding pathways of bovine pancreatic ribonuclease A (RNase A)[1] when the reduced protein is treated with oxidized dithiothreitol (DTT^{ox})[1] (*1*−*3*). Native RNase A contains four disulfide bonds, at positions [26−84], [40−95], [58−110], and [65−72], and kinetic studies (*2*) have led to the mechanism illustrated in Figure 1. The species *n*S are ensembles[2] of n disulfide bonds, there being 28, 210, 420, and 104 theoretically possible species, with $n = 1$, 2, 3, and 4, respectively, in addition to the fully reduced (R) and completely folded (N) forms. The ensembles R and *n*S attain a preequilibrium steady state, after which one or more species in the 3S ensemble undergo a disulfide-exchange reaction to form des-[40−95][1] and des-[65−72][1] in rate-determining steps, and then these species convert rapidly to N; both des-[40−95]

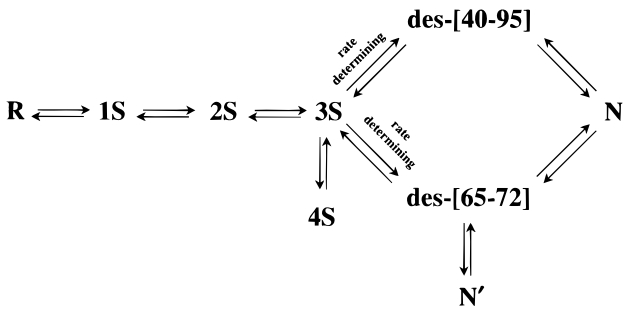

FIGURE 1: Regeneration pathways of disulfide-reduced and denatured RNase A by oxidation with DTT^{ox} at 25 °C and pH 8.0 (*2*). R indicates the fully reduced protein, *n*S indicates species with n disulfide bonds, the des-species contain three native disulfide bonds and lack the bond indicated in brackets, N is the native protein, and N′ is a cyclic nativelike adduct of des-[65−72] with DTT (3).

† This work was supported by the National Institute of General Medical Sciences of the National Institutes of Health (Grant GM-24893). Support was also received from the National Foundation for Cancer Research.

* To whom correspondence should be addressed. Phone: 607-255-4034. Fax: 607-254-4700. E-mail: has5@cornell.edu.

‡ M. Volles was a Howard Hughes Summer Research Scholar, summer 1997.

§ X. Xu was a Leukemia Society of America Special Fellow, 1995-1997.

[1] Abbreviations: AEMTS, 2-aminoethylmethanethiosulfonate; BPTI, bovine pancreatic trypsin inhibitor; CFIS, chain-folding initiation site; des-[40−95], des-[65−72], folding intermediates of RNase A containing three native disulfide bonds but lacking the disulfide bond in brackets; DDS, disulfide detection system; DTT^{ox}, oxidized dithiothreitol; DTT^{red}, DL-dithiothreitol (reduced dithiothreitol); EDTA, ethylenediaminetetraacetic acid; GdnSCN, guanidine thiocyanate; Hepes, 4-(2-hydroxyethyl)-1-piperazineethanesulfonic acid; HPLC, high-performance liquid chromatography; MALDI-TOF, matrix-assisted laser desorption ionization-time-of-flight; MS, mass spectrometry; nS, a folding intermediate or ensemble of folding intermediates with n disulfide bonds; NTSB, disodium 2-nitro-5-thiosulfobenzoate; RNase A, bovine pancreatic ribonuclease A; TFA, trifluoroacetic acid; Tris, 2-amino-2-(hydroxymethyl)-1,3-propanediol.

[2] A *disulfide species* is defined as a protein with a particular set of disulfide bonds, while a *disulfide ensemble* consists of all the disulfide species with the same number of disulfide bonds. For example, des-[40−95] is a single disulfide species in the 3S ensemble. Thus, redox reactions are interconversions among disulfide ensembles, e.g., 1S → 2S, while disulfide reshuffling reactions are interconversions among disulfide species within an ensemble, e.g., [65−84] → [65−72] in the 1S ensemble.

10.1021/bi990570f CCC: $18.00
Published on Web 05/13/1999

and des-[65−72] contain three native disulfide bonds. Almost 80% and 20% of the native protein is regenerated through the des-[40−95] and des-[65−72] pathways, respectively (*2*); experiments with mutants (*4*, *5*) suggest that the wild-type protein also uses minor pathways (to the extent of about 3−5% each) in which the rate-determining step is the formation of des-[40−95] and des-[65−72], respectively, by oxidation of species in the 2S ensemble.

To characterize the folding pathway(s) completely, it is necessary to determine the distribution of species in each of the *n*S ensembles. The distributions provide information about the differences in free energy among the species within an ensemble and, hence, about the intramolecular interactions that determine the distributions; those interactions *may* persist among more highly oxidized species along the folding pathway. Thus far, the 1S ensemble has been characterized, and 40% of the 28 theoretically possible one-disulfide species have been found to have the native [65−72] bond, 10% have the nonnative [58−65] disulfide bond, and the 26 remaining one-disulfide species are all present to the extent of less than 10% each (*6*). The dominance of the [65−72] disulfide bond (to an extent that is 2.4 times the amount expected from reduction of entropy by loop formation) implies the presence of energetic interactions that stabilize this loop; in fact, this loop has been proposed as one of several chain-folding initiation sites (CFIS)[1] that promote further folding of this protein by restricting the available conformational space (*7*).

This paper is concerned with the distribution of disulfide bonds in the 2S ensemble. It should be noted that the experiments to determine the 2S distribution are much more complicated than those used in determining the 1S distribution because of the presence of 210 possible species in the 2S ensemble compared to 28 in the 1S ensemble. Therefore, in this initial investigation of the 2S ensemble, we have confined our approach to determining the distribution of one-disulfide bonds among the 2S species. The resulting data provide an experimental basis for ultimately probing the role of intramolecular interactions within the species of the 2S ensemble in the folding pathway(s).

MATERIALS AND METHODS

Materials. RNase A (type 1-A, Sigma Chemical Co.) was purified as described previously (*8*). DTT^{ox} (Sigma Chemical Co.) was purified as described by Creighton (*9*). DTT^{red} was purified by isocratic reversed-phase HPLC [3% acetonitrile, 0.05% TFA, YMC minibore column (ODS AQ 120A S3, 2 × 150 mm)] and stored at −70 °C. AEMTS[1] was prepared by the method of Bruice and Kenyon (*10*). NTSB[1] was prepared by the method of Thannhauser et al. (*11*). Trypsin (type III, from bovine pancreas) and α-chymotrypsin (type II, from bovine pancreas) were obtained from Sigma Chemical Co. All other reagents were of the highest grade commercially available.

Reduction and Regeneration of RNase A. RNase A was fully reduced by the method of Xu et al. (*6*). The protein was regenerated at a concentration of 25 μM in a solution of DTT^{ox} (initial concentration of 80 mM), Tris (100 mM, pH 8.0), and 2 mM EDTA. The solution was sparged with argon prior to the addition of DTT^{ox} or protein. The reaction was allowed to proceed at 25 °C under an atmosphere of argon for 30 min, at which time AEMTS was added to a concentration of 20 mM (a 100-fold molar excess over free thiols). This blocking process was allowed to proceed at room temperature for 5−10 min, after which the pH was lowered to between 4 and 5 with acetic acid. The mixture was either frozen at −70 °C or injected immediately onto an HPLC column for purification.

Isolation of Two-Disulfide Intermediates. The quenched regeneration mixture prepared above was injected onto either a semipreparative or an analytical cation-exchange HPLC column [Rainin Hydropore-5-SCX (10 mm × 10 cm) or (4.6 mm × 10 cm)]. The following gradient was used: 100% buffer C (50 mM acetic acid, pH 5.0) was run for 10 min to elute nonprotein species. Then, within 2 min, the gradient was changed to 89% buffer A (25 mM Hepes, 1 mM EDTA, pH 7.0), 11% buffer B (buffer A + 1 M NaCl), and held for 10 min. Buffer B was then increased to 22% over 40 min. The HPLC system was a series 1100 from Hewlett-Packard corporation, and UV absorption was monitored at 280 nm. The fraction corresponding to the 2S intermediates was collected and dialyzed against 4 L of 100 mM acetic acid at 4 °C for 36 h. The 4 L of acetic acid was changed 3 times during the 36 h at approximately equal intervals. The dialyzed protein solution was lyophilized and reconstituted into 100 mM acetic acid (at an RNase A concentration of approximately 2 mg/mL) and stored frozen at −70 °C. The purity of the 2S species was checked by reinjection onto an HPLC column. No impurities were detected throughout the course of the experiments.

Proteolytic Digestion. Digestion of the isolated two-disulfide intermediates, and also reduced and AEMTS-blocked RNase A (as a standard), was carried out in preparation for peptide mapping. The protein was diluted to a concentration of 0.5 mg/mL in 100 mM Tris, 2 mM EDTA, at pH 8.0 and 25 °C. Digestion was first carried out with trypsin (at an enzyme/substrate mass ratio of 1/50) for 1 h and then with α-chymotrypsin at the same concentration for another 1 h. The pH of the solution was then lowered to 2 with 20% (v/v) TFA. The digested mixture was stored at −70 °C.

Peptide Mapping. The digests were analyzed using reversed-phase HPLC (with a Hewlett-Packard series 1100 system, with a binary pump and a diode array detector). Absorbance was monitored at 215 nm. A YMC minibore column (ODS AQ 120A S3, 2 × 150 mm) was used with a binary gradient. First, 94% buffer A (100% H_2O, 0.05% TFA) and 6% buffer B (50% acetonitrile, 0.05% TFA) was run isocratically (0.2 mL/min) for 10 min, followed by a change to 65% B over a 100 min period. All digestion fragments eluted within this gradient range.

All peaks from both the reduced-blocked (standard) and two-disulfide digestion chromatograms were collected and lyophilized separately and subjected to MALDI-TOF mass analysis. The mass spectrometer used was from Finniganmat (Lasermat model 2000). Samples were prepared by dissolving the lyophilized fragments collected above in 3 μL of 0.05% TFA. The matrix used for MALDI-TOF analysis contained 70% acetonitrile with 10 mg/mL α-cyano-4-hydroxycinnamic acid. The masses determined with this instrument have an error of less than 0.1%.

Disulfide Bond Analysis. The amount of material in the disulfide-containing fragments from the HPLC chromatograms of both the reduced-blocked (standard) and two-

disulfide protein digestions was determined quantitatively. A disulfide detection system (DDS), developed by Thannhauser et al. (*12*), was connected in series with the UV detector. This system consisted of a solution (0.5 M Na_2SO_3, 2 mM EDTA, 0.5 mM NTSB, 200 mM glycine, pH 9.5) pumped isocratically (HP1100, quaternary pump, 0.5 mL/min) to a tee fitting, which mixed this solution with effluent from the detector of the reversed-phase HPLC system. The mixed solution then proceeded through a 30 s reaction loop (0.01 in. i.d.) to the detector (HP1100 variable wavelength, 410 nm) The signal from the DDS detector is proportional to the number of moles of disulfide bonds eluting at a given time. Therefore, the concentrations of peptides can then be determined quantitatively based on the number of disulfide bonds that they contain.

Reduction and Reblocking. In addition to a mass spectral analysis of each lyophilized fraction from the two-disulfide digestion chromatogram, a reduction and reblocking process was also carried out. This is necessary in order to determine the composition of each fraction quantitatively, because most of the fractions from the HPLC chromatogram each contain several fragments. The reduction and reblocking method also serves to confirm the mass spectral analysis.

The lyophilized digestion fragments were resuspended in 20 μL of Tris (100 mM, pH 8.0), then purified DTT^{red} ($\sim$7 mM, 10 μL) was added, and reduction was allowed to proceed for 30 min, after which the solution was quenched with AEMTS (freshly dissolved in water, 10 mM, 30 μL). After 5−10 min, the pH of the solution was adjusted to 5.0 with 1 M acetate buffer. The resulting samples were stored at −20 °C until they could be injected onto an HPLC column. The HPLC gradient and system used for this purpose was the same as that described in the Peptide Mapping section. The resulting fragments were identified by comparison with the retention times of the digested fragments of reduced and blocked RNase A. The relative abundance of each fraction was determined by the disulfide detection system.

The entire set of experiments was carried out twice. Within each experiment, DDS quantitative analysis of the peptide map from the enyzmatically digested protein was repeated at least twice. The experiment was also repeated a third time without carrying out the reduction and reblocking experiments. The average of the standard deviations of the 28 one-disulfide percentages from the two independent experiments was 0.2. To validate the experimental method further, the fraction of the total DDS signal in a peptide map due to intrapeptide (intra- with respect to the 2S species *prior* to tryptic/chymotryptic digestion) disulfide bonds (as opposed to peptide-AEMTS blocked disulfide bonds) was determined. Since a 2S intermediate contains two disulfides and four blocked cyteines, the intrapeptide disulfide bonds should make up 2/6 of the DDS signal, or 33%. The experimental value for the total intrapeptide disulfide content agreed with this estimate to within 5% in each experiment.

RESULTS

Regeneration Experiments. The kinetics and thermodynamics of RNase A regeneration have been studied extensively (*1*, *2*, *8*, *13*). Using these kinetic data, the regeneration time, DTT^{ox} concentration, and protein concentration were chosen to produce a maximum yield of 2S intermediates

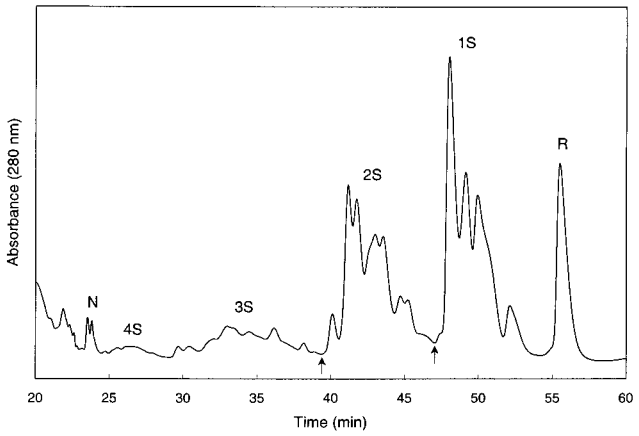

FIGURE 2: Ion-exchange chromatogram from a typical regeneration experiment using 80 mM DTT^{ox}, 25 μM reduced RNase A, pH 8.0, 25 °C, and AEMTS blocking, at 30 min. R indicates fully reduced protein, *n*S indicates species with n disulfide bonds, and N indicates the native protein. Arrows bound the fraction containing the 2S intermediates that was collected and used in further experiments. Peaks eluting before N do not contain protein and arise from salts used in the regeneration/blocking process.

($\sim$40% of the total protein). In this experiment, it is not necessary to allow the regeneration to reach the steady state before quenching the reaction since the intragroup disulfide distribution is nearly invariant with respect to regeneration time (*13*). This is because the rate of intramolecular disulfide reshuffling is 2−4 orders of magnitude greater than the rates of oxidation and reduction between disulfide groupings under the redox conditions used in this experiment (*13*). A typical cation-exchange chromatogram of the blocked regeneration mixture is presented in Figure 2. Because of the positive charge added to each of the free protein thiols after blocking with AEMTS, the disulfide groupings are well separated using cation-exchange HPLC. The chromatogram observed here is similar to those reported previously, and the peak assignments that are labeled in the figure have been identified previously (*6, 8*).

Peptide Mapping. A tryptic, α-chymotryptic digestion map of AEMTS-blocked RNase A has been reported previously (*6*). The typical trypsin/chymotrypsin cleavage sites as well as two atypical cleavage sites were observed here as well as in that work: one between Met 79 and Ser 80 and the other following blocked Cys 110. The map in the experiments reported here agrees with that of Xu et al. (*6*) and adds the observation of one additional cleavage site (observed to occur less than 10% of the time) following blocked Cys 58. The cleavage after blocked cysteine is probably due to the analogous structures between lysine and this residue (*6*).

The digestion map monitored by UV absorption and the corresponding DDS chromatogram (used as a measure of the concentrations of disulfide-containing peptides) of the digested 2S intermediates are displayed in panels a and b of Figure 3, respectively. Each peak in the DDS map containing disulfide-bonded peptides is labeled, and Table 1 lists the corresponding peak compositions, along with their observed and calculated masses. Each identity was determined by matching a table of theoretically possible masses to the observed mass, and the identities were confirmed by reduction and reblocking experiments, as outlined in the Materials and Methods and discussed below.

Table 1: Tryptic-Chymotryptic Digestion Fragments of the 2S Intermediates[a]

peak	observed mass[b]	assignment[c]	expected mass[d]	disulfide[e]	percent of total disulfides[f]	peak	observed mass[b]	assignment[c]	expected mass[d]	disulfide[e]	percent of total disulfides[f]
a	1287	(26−31, 62−66)	1289	[26−65]	1.05	m	1873	(38−46, 67−73)	1881	[40−72]	0.40
b	1335	(62−66, 67−73)	1335	[65−72]	26.14		1662	(40−46, 92−98)	1666	[40−95]	0.66
c	1227	(62−66, 80−85)	1226	[65−84]	1.68	n	2146	(47−61, 62−66)	2148	[58−65]	6.22
	1314	(62−73)	1317	[65−72]	0.61	o	2371	(26−31, 47−61)	2370	[26−58]	2.22
d	1448	(26−31, 80−85)	1448	[26−84]	2.23		1608	(40−46, 67−73)	1609	[40−72]	1.48
	1983	(62−66, 86−98)	1981	[65−95]	0.22	p	1749	(62−66, 105−115)	1750	[65−110]	0.93
	1715	(62−66, 67−76)	1714	[65−72]	0.45	q	3065	(47−61, 86−98)	3062	[58−95]	0.95
	1393	(62−66, 92−98)	1392	[65−95]	0.45		2312	(47−61, 80−85)	2308	[58−84]	2.29
e	1489	(67−73, 80−85)	1494	[72−84]	1.69		1972	(26−31, 105−115)	1971	[26−110]	1.53
	1608	(26−31, 92−98)	1613	[26−95]	0.89		2414	(47−61, 67−73)	2416	[58−72]	4.77
	2200	(26−31, 86−98)	2202	[26−95]	0.20	r	2668	(86−98, 105−115)	2664	[95−110]	0.73
	1552	(26−31, 67−73)	1556	[26−72]	1.43		2475	(47−61, 92−98)	2473	[58−95]	0.87
f	1339	(40−46, 62−66)	1342	[40−65]	0.85		1908	(80−85, 105−115)	1909	[84−110]	1.73
	ND[g]	(38−46, 62−66)	1613	[40−65]	0.25		1808	(38−46, 86/92−97)[i]	1809	[40−95]	0.14
g	1551	(80−85, 92−98)	1551	[84−95]	8.07	s	1539	(40−46, 92−97)	1538	[40−95]	0.27
	2145	(80−85, 86−98)	2140	[84−95]	2.77	t	2075	(92−98, 105−115)	2074	[95−110]	2.18
	2251	(67−73, 86−98)	2249	[72−95]	0.84		2013	(67−73, 105−115)	2017	[72−110]	2.41
h	1658	(67−73, 92−98)	1659	[72−95]	1.27		2938	(47−61, 86−97)	2934	[58−95]	0.14
i	1550[h]	(67−73, 92−97)	1531	[72−95]	0.72	u	2421	(40−46, 47−61)	2423	[40−58]	1.42
j	2012	(80−85, 86−97)	2012	[84−95]	0.45		2693	(38−46, 47−61)	2694	[40−58]	0.70
	1482	(26−31, 92−97)	1485	[26−95]	0.35	v	2342	(47−61, 92−97)	2345	[58−95]	0.42
k	1423	(80−85, 92−97)	1423	[84−95]	1.11		2533	(86−97, 105−115)	2535	[95−110]	0.17
	1498	(40−46, 80−85)	1501	[40−84]	1.52		2627	(47−61, 77−85)	2627	[58−84]	0.17
	1769	(38−46, 80−85)	1772	[40−84]	0.89	w	2295	(38−46, 105−115)	2295	[40−110]	0.55
l	1560	(26−31, 40−46)	1563	[26−40]	6.69	x	2024	(40−46, 105−115)	2024	[40−110]	1.10
	1936	(38−46, 92−98)	1937	[40−95]	0.20		1945	(92−97, 105−115)	1946	[95−110]	0.48
	1810	(67−73, 77−85)	1814	[72−84]	0.36		2079	(40−46, 47−58)	2078	[40−58]	0.36
						y	2829	(47−61, 105−115)	2831	[58−110]	1.34

[a] Peak labels correspond to the labeled peaks in the digestion chromatogram of Figure 3b. [b] The experimentally determined mass. [c] The amino acid residues making up the peptides in this peak. Two sets of fragments in parentheses, separated by a comma, indicates that these two peptides are joined by a disulfide bond. A single peptide in parentheses indicates that this peptide has an intramolecular disulfide bond. Only peak components containing intrapeptide disulfide bonds are listed. [d] The theoretical mass for the fragment listed, based on an average isotopic distribution. [e] The cysteine residues forming the disulfide bond. [f] The contribution that each component makes to the total intrapeptide disulfide distribution. Data are from one of two experiments. The experiments produced data with an average standard deviation in the percentage of 0.2 (see text). [g] ND indicates that this mass was not observed experimentally, but the peptide was clearly seen in the reduction and reblocking experiments. [h] The experimentally determined mass differs significantly from the expected value, possibly because of bound Na^+ during MS. Reduction and reblocking studies conclusively identified the peptide. [i] This peak contained both (38−46, 86−97) and (38−46, 92−97), which were not distinguished chromatographically after reduction and reblocking, because of their close elution position and their equivalent disulfide bond.

As a control experiment, a digestion was carried out in the absence of RNase A. This digestion mixture was injected onto an HPLC column to determine if any of the peaks in Figure 3a arise from autodigestion fragments of trypsin and/or α-chymotrypsin. No significant peaks were observed. This is to be expected, since the protease/RNase A ratio during the digestion was 1/50.

Peak Component Analysis. Since many of the peaks identified in the mapping part of the experiment contain multiple species, the relative amounts of each component within each peak were determined using the reduction and reblocking procedure. Fractions from the 2S digestion map, shown in Figure 3b, were collected, reduced, and then reblocked with AEMTS. The resulting peptides were then examined with reversed-phase HPLC coupled to the DDS, exactly as in the peptide-mapping experiments. The peaks observed were characterized by their retention times, in comparison to the reduced and digested protein (standard) map. In this way, the identities of the disulfides in a fraction could be confirmed and the relative concentrations of the species could be determined. The identities could be found because two peptide fragments that are joined by a disulfide bond will exhibit the same DDS peak areas when rechromatographed after reduction and reblocking with AEMTS. The identity determined in this way confirmed the mass spectral analysis of the digestion map obtained earlier. However, the DDS analysis serves only as a verification of the MS data and is not the primary method of peak identification.

As mentioned above, the DDS peak areas are also a direct measure of the relative concentration of each species within a digestion fraction, since each area is directly proportional to the molar quantity of disulfide bonds present in that peak. However, it should be noted that any DDS peak area corresponding to a fragment that contained an intrapeptide disulfide intermediate in the original peak (prior to reduction and reblocking) must be divided by a factor of 2 when compared to the area from (original) AEMTS-blocked species. This is because an intrapeptide disulfide intermediate, after reduction and reblocking, forms two disulfide bonds (from the two blocked cysteines), and thus, its DDS area will be greater than the original molar quantity of the intermediate by a factor of 2. This issue is of concern with those fractions that contain both intrapeptide disulfides and AEMTS-blocked peptides.

One experimental concern is that the short reaction time of the DDS (30 s.) may be insufficient to allow the reaction to reach completion before reaching the detector. Under the conditions used, the reaction is pseudo-first-order (unpublished results), and therefore, an incomplete reaction will not

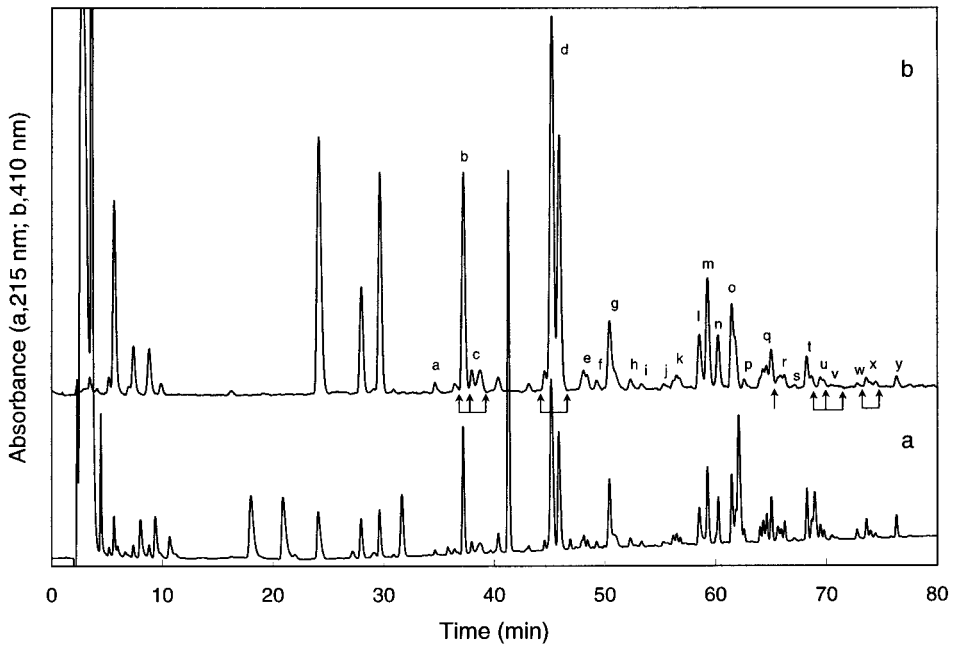

FIGURE 3: A typical reversed phase HPLC chromatogram of the two-disulfide intermediates after tryptic/chymotryptic digestion. The bottom chromatogram (a) shows the UV absorbance at 215 nm, and the top (b) shows the corresponding DDS signal. Letters denote peaks that contain intrapeptide disulfide bonds, and correspond to the letters used in Table 1. Unlabeled peaks contain either AEMTS blocked protein only, or no disulfide bonds at all. Arrows indicate the starting/stopping point of collection for a given peak. The arrows are drawn only in positions where peak fractionation might otherwise be ambiguous. Likewise, connected arrows are drawn in ambiguous cases to delineate the contents of a given labeled peak precisely.

affect the relative proportions of the integrated peak areas, unless different peptides react with different rate constants. Furthermore, in repetition of the experiments using more concentrated DDS reagents, the results did not change significantly (unpublished results), indicating that the peptides react rapidly enough, and the 30 s reaction time is sufficient for analysis of the disulfide species.

The results of the peak component analysis of the enzymatic digestion fragments are shown in Table 1. The components of each intrapeptide disulfide-containing fraction are listed (labels correspond to those used in Figure 3b). Many of the 28 possible disulfide bonds have multiple entries in Table 1, because of incomplete cleavage at some digestion sites. While this complicates the experiments, it does not affect the results in any way.

The total experimental abundance for each of the 28 possible single-disulfide bonds is shown in Table 2. These abundances were obtained by adding the percent abundances of all entries in Table 1 which correspond to a given disulfide bond. It is interesting that all 28 disulfide bonds were observed to be present in the 2S intermediates during folding, and that many of these disulfides have relatively small abundances (<5%). An exception to this is the native disulfide bond [65−72], which is observed to make up 27% of the total single-disulfide bonds. As discussed below, this implies that over 50% of the 2S intermediates contain bond [65−72]; this large percentage may have significant implications for the folding process.

DISCUSSION

Entropy Loss Due to Disulfide-Bond Formation. As a preliminary investigation of the 2S ensemble, we have determined the distribution of disulfide bonds in the 2S intermediates. The population of any 2S intermediate is proportional to $\exp(-\Delta G^\circ/RT)$, where ΔG° is the standard Gibbs free-energy difference between peptides with and without two disulfide bonds. The part of direct interest for the present analysis is the intramolecular enthalpy-change component of ΔG°, which is a direct measure of the net change in potential energy in forming a set of conformations with the imposed two-disulfide constraints from a disulfide-reduced molecule. A qualitative measure of the intramolecular enthalpy change involved in forming a specific disulfide bond may be obtained by examining the ratio of the experimentally determined abundance of a disulfide-containing species to the abundance that is predicted based only on entropy contributions to the free energy change.[3] The required entropy changes are calculated theoretically by using the following equation (eq A-10 of ref *14*), which is based on a random-flight statistical mechanical model (*14-16*) and on the Wang−Uhlenbeck expression for multivariate Gaussian distributions:

$$\Delta S^\circ = R(-3.47n + 3n \ln a - 1.5 \ln|C|) \qquad (1)$$

where R is the gas constant, a is the length of a chain element, n is the number of disulfide bonds (two in this

[3] It should be noted, however, that the ratio obtained in this manner is arbitrary in an absolute sense. Each ratio for a specific disulfide species is meaningful only relative to the ratios determined for the other disulfide species. This is because the portion of the enthalpy change for disulfide-bond formation due to the intermolecular redox chemistry, assumed to be the same for all disulfides, cannot be accounted for in the calculations, introducing an unknown constant proportionality factor into each theoretically predicted concentration. This proportionality factor cancels out when comparing ratios relative to each other. Likewise, it would not be possible to discern a constant intramolecular enthalpy change that occurred in the formation of every disulfide species, because this constant energy change would be absorbed into the arbitrary constant associated with the redox chemistry.

Table 2: Experimental Results for the Distribution of One-Disulfide Bonds in the 2S Intermediates, and Comparison with Theory

disulfide[a]	experimental percentage[b]	theoretical percentage[c]	ratio[d]	ratio in 1S[e]
26−40	6.6	8.4	0.8	0.7
26−58	2.4	1.9	1.3	1.5
26−65	1.0	1.3	0.8	ND
26−72	1.4	1.3	1.1	ND
26−84	**2.2**	**1.1**	**2.0**	**1.8**
26−95	1.3	1.0	1.3	2.2
26−110	1.8	0.8	2.3	2.5
40−58	2.4	4.3	0.6	0.6
40−65	1.1	2.3	0.5	0.6
40−72	1.9	2.0	1.0	0.5
40−84	2.3	1.6	1.4	ND
40−95	**1.2**	**1.3**	**0.9**	**1.5**
40−110	2.0	1.0	2.0	3.6
58−65	5.9	12.8	0.5	0.6
58−72	4.7	4.4	1.1	1.1
58−84	2.3	2.7	0.9	1.0
58−95	2.3	1.9	1.2	0.4
58−110	**1.2**	**1.3**	**0.9**	**1.9**
65−72	**26.6**	**11.9**	**2.2**	**2.4**
65−84	1.7	3.0	0.6	ND
65−95	0.7	2.0	0.4	0.6
65−110	1.0	1.2	0.8	0.6
72−84	2.1	6.7	0.3	0.3
72−95	3.3	2.8	1.2	1.1
72−110	2.3	1.6	1.4	1.5
84−95	12.9	9.7	1.3	1.0
84−110	1.8	2.8	0.6	0.1
95−110	3.7	7.0	0.5	0.7

[a] The disulfide pairing of each of the 28 possible disulfide linkages. Disulfide bonds present in the native state are shown in boldface type. [b] The experimentally determined value for the percent of total disulfide bonds having the listed bond. This value is an average of the values from two independent experiments. [c] The theoretically predicted value for the percent of the listed disulfide, based on eqs 1 and 2, as described in the text. Also see footnote 3. [d] Ratio of the experimentally determined percentage to the theoretically predicted percentage. [e] The ratios found previously for the 1S intermediates (*6*). ND indicates that this bond was not observed experimentally.

study), C is a (2×2) symmetric matrix whose elements are C_{ij} = (number of residues shared by loops i and j) $\times$ (a^2), and $|C|$ is the determinant of C (*14*). The constant a cancels out in eq 1, and therefore, its numerical value is not needed for the calculations.

Equation 1 provides the entropy of formation of any specific topology of two-disulfide bonds (either independent or overlapping) from the fully reduced protein. Disulfide-bond formation always results in a decrease in entropy of the protein since an intramolecular bond restricts the conformational space available to the chain. Intuitively, it is clear that two distant regions connected by a bond will have a greater entropy loss than a bond formed from near neighbors, and this is reflected in eq 1. Likewise, multiple bonds increase the entropy loss to an even greater extent. However, if two intramolecular bonds overlap (are dependent), then less entropy is lost in their formation, than if they did not share part of the chain. This is because formation of the second bond of a pair, in a region already involved in a loop, provides less restriction on the number of conformations accessible to the chain because the chain was already conformationally restricted by the first bond. Yet, if the second bond formed in a region not already involved in a loop, the entropy loss would have been greater because that region was not restricted conformationally to begin with (*16*). This effect is accounted for in the entropy calculations presented above: if there are no overlapping loops, the off-diagonal entries of C_{ij} become zero.

If ΔH_i° were a constant, the predicted relative abundance of a given two-disulfide intermediate$_i$ (I_i) at equilibrium would be calculated by using the entropy change ΔS_i° from eq 1 as follows, for all 210 possible two-disulfide intermediates:

$$[I_i] \propto \exp(\Delta S_i^\circ / R) \qquad (2)$$

A proportionality constant is not needed since the concentrations of the 2S intermediates need to be calculated only relative to each other.

The experimental data obtained in this work are percent abundances of the 28 possible single disulfide bonds: single because disulfide-bond pairs that originally exist in a 2S intermediate are decoupled into single disulfide bonds during tryptic/chymotryptic digestion. Thus, the percent abundance of any single disulfide bond actually consists of the sum of the percent abundances of the 15 2S intermediates that contain that bond, because each of the 28 possible single disulfide-bonds can be combined with one of 15 distinct disulfide bonds to form a 2S intermediate.

It is of interest to compare the experimental data for these 28 single disulfide abundances with the entropy calculations for all 210 theoretically possible 2S intermediates given by eqs 1 and 2. To do this, we must compute a sum for each of the 28 possible one-disulfides, with each sum consisting of 15 terms, those being the abundances (from the 210 calculations) of each possible 2S intermediate that could form from the given one-disulfide, just as the experimental data represent sums (over 15 2S intermediates each), as described above. For example, a 1S intermediate with, say, a disulfide bond [26−40] can form one of 15 possible second disulfide bonds with its six remaining cysteines, to form one of 15 distinct 2S intermediates containing bond [26−40]. As described above, the experimental result for the abundance of bond [26−40] is the sum of the abundances of all 15 of the 2S intermediates containing it. Likewise, the abundances of all 15 2S intermediates containing bond [26−40] were calculated with eqs 1 and 2 and are added together, producing a theoretical value that can be compared directly with the experimental value.

Distribution of Disulfide Bonds in the 2S Intermediates. The results of the experimental measurements and theoretical calculations for each of the 28 single disulfide bonds are displayed in Table 2, along with the ratio of these two figures. The ratio for each bond in the 1S distribution as determined by Xu et al. (*6*) is also shown for reference. All 28 possible disulfide bonds were observed in this study, and many of the bonds are present at only low levels (<5% each for 24 of 28 possible bonds). The four bonds with levels greater than 5% ([26−40], [58−65], [65−72], and [84−95]) are all involved in relatively small disulfide loops. Since, with the exception of bond [65−72], these four relatively abundant disulfide bonds have ratios that do not differ greatly from the average of the ratios of the other disulfide bonds, they are probably stabilized relative to the other disulfides predominantly by entropy. For [58−65] and [65−72], the

theoretical percentages are almost the same[4] (same size loops), indicating similar entropic contribution; hence, the differences in experimental percentages must be due to enthalpic contributions. It should be noted that bond [65−72] accounts for 26.6% of the total population and, therefore, is present in ∼53% of all 2S intermediates, because each 2S intermediate contributes not one, but two, disulfide bonds to the experimental data. For example, if [65−72] were present in every 2S intermediate that formed during folding, the abundance measured in this experiment would be only 50%, because the amount of [65−72] would be weighed against all of its disulfide partners. The only other bond that has an experimental abundance above 10% is [84−95].

The ratios determined in this study (Table 2) and those determined for disulfide bonds in the 1S distribution [Table 2 (*6*)] are well correlated (correlation coefficient, *R*, equals 0.83). This indicates that the 2S and 1S species probably contain similar energetic interactions, on average. These results and their implications will be discussed in more detail below.

The 2S Intermediates Are Globally Disordered. All of the 28 possible one-disulfide bonds are observed to be present in the ensemble of 2S intermediates, as shown in Table 2. If a few specific disulfide bonds tended to pair together to form especially favorable 2S intermediates, one would expect to see a few dominating experimental abundances in Table 2, arising from these energetically favored pairings. Although some disulfide bonds do have large experimental percentages, the highest percentage possibly attributable to a single two-disulfide intermediate is ∼26% (which is twice the experimentally determined percentage of [84−95] shown in Table 2) in the extremely unlikely event that bond [84−95] was paired only with [65−72]. This event is unlikely because it implies the existence of nonnative stabilizing interactions in the intermediate containing [65−72] and [84−95] and destabilizing nonlocal interactions in most of the other 14 possible two-disulfide species containing [84−95], since the [84−95] ratio is not significantly larger than the ratios for other disulfides.

Since all 28 one-disulfide bonds are observed in significant quantities (Table 2), a similar argument indicates that a substantial number of the 210 possible 2S intermediates are likely to be present at significant levels during folding. While the alternative, that only a limited number of 2S species are present (at least 14, since all 28 one-disulfide bonds were observed), is possible, it would require that these species be specifically much more stable than the other possible 2S intermediates. This specificity would require specific long-range interactions, and these interactions would in general be nonnative, since most of the species would have non-native disulfide bonds. It is difficult to envision that such specific, non-native, long-range stabilizing interactions could actually be present in each of the cases (at least 14) necessary to give rise to all 28 one-disulfide bonds. Furthermore, such an alternative would imply the presence of strong enthalpic dominance of the thermodynamic distribution and, thereby, would not explain the correlation between the observed disulfide levels and the entropy-based predictions of theoretical abundance (Table 2) by any plausible mechanism. Therefore, it can be concluded that the 2S intermediates are not dominated by a small number of highly stable, structured intermediates, but rather that many globally disordered 2S intermediates are present, in a distribution dominated by entropy and local (i.e., pertaining to single disulfide loops) enthalpy factors. By contrast, only a few 2S intermediates were observed in the folding of BPTI (*17*). Further evidence for these conclusions comes from spectroscopic (*18*, *19*) and kinetic (*2*, *13*) measurements and urea-gradient electrophoresis in parallel with other assays (*20*), showing that the RNase A folding intermediates are globally disordered. However, specific 2S intermediates that are stabilized to a lesser extent cannot be ruled out with the data from these experiments. The implications of this observation for folding will be discussed below.

The absence of specific long-range interactions in the 2S intermediates is in striking contrast with studies of BPTI, whose folding pathway has been shown to be directed by predominantly native interactions (*17*), with almost complete folding occurring with the formation of a single disulfide bond [5−55] (*21*) or [30−51] (*22*). Because of the small size and unusually high stability of BPTI, it is likely that the more disordered intermediates observed in the folding of RNase A represent a more general case.

One other point to address is the recent discovery of a cyclic nativelike adduct of DTT with RNase A, designated N′, formed during the oxidation of des-[65−72] (*3*). The existence of a similar DTT adduct in the 2S species is a possibility, although it is believed that the formation of N′ hinges on specific structural effects present in des-[65−72], a three-disulfide intermediate missing the [65−72] disulfide bond (*3*). The largely disordered structure present in the 2S intermediates, as demonstrated above and in refs *8* and *18*−*20*, makes the formation of a 2S N′ analogue unlikely. Even if any N′ analogue does indeed form, the amount will be too small to change the conclusions of this study.

The 2S and 1S Intermediates Are Probably Compact. A hydrophobic collapse is often thought to be an integral part of the early stages of protein folding. If the 2S intermediates are collapsed, this should be observable in the disulfide-bond distribution, because a collapse would enhance the stability of larger disulfide loops (including [26−84], [58−110], and [40−95], which are found in the native state) with respect to smaller loops relative to a statistical coil. Formation of a large loop in a *compact* protein is more energetically favorable than in a noncompact protein, because less entropy is lost in the formation of the loop, if the protein is already compact. In Figure 4, the ratio of experimental to theoretical abundance of one-disulfide bonds (from Table 2) is plotted against the loop length. The regression line of Figure 4 has a positive slope which shows that longer disulfide loops are indeed more favored than one would expect based on calculations with eqs 1 and 2 or that shorter disulfide loops are less favored than would be expected. In the absence of this trend, the regression line would have a slope of zero.[5]

It could be argued that the observed trend in Figure 4 is completely due to the enthalpic stabilization of [65−72]

[4] As *isolated* [65−72] and [58−65] loops, the entropic contributions would be the same. However, as overlapping loops, with the percent abundance of a single disulfide bond being calculated as the sum of the percent abundances of the 15 2S intermediates that contain that bond, the entropic contributions of these two equal-size loops are not exactly the same.

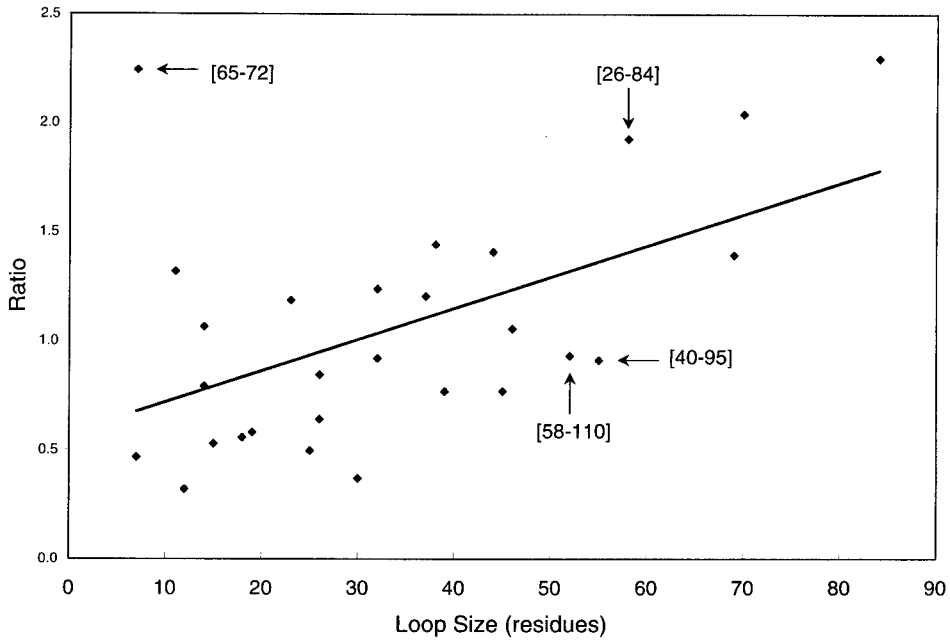

FIGURE 4: The ratio of experimental to theoretical abundance (from column "ratio" of Table 2) for each possible disulfide bond as a function of the size of the disulfide loop, i.e., the number of amino acid residues. The four data points corresponding to native disulfide bonds are labeled. The slope of the regression line is 0.014, with $R^2 = 0.28$ (R is the correlation coefficient).

(discussed below), since on average, a single disulfide in a 2S intermediate that could have [65−72] as one of its 15 possible partners is longer than a disulfide that could not have [65−72] as one of its 15 partners (i.e., a disulfide containing either Cys 65 or Cys 72). This follows from the fact that [65−72] is in the middle of the protein, and therefore, a disulfide which pairs with it is more likely to stretch the length of the protein. While it is to be expected that some of the slope of the trendline in Figure 4 is produced by this phenomenon, the following evidence suggests that it cannot completely account for it.

If this phenomenon could account completely for the observed trend, then, by distinguishing in Figure 4 between disulfides that could and those that could not pair with [65−72], we should be able to identify two sets of data points; each set would have a trendline of approximately zero slope[5] (because the [65−72] phenomenon could not cause a nonzero slope in the two *separate* data sets), and with an average *y*-coordinate (ratio) of those bonds that could pair with [65−72] greater than the average *y*-coordinate of those that could not. Indeed, the average ratio for those bonds that could be paired with [65−72] in a 2S intermediate is 1.2 whereas the average for those bonds that could not (excluding bond [65−72] itself) is 0.8, a difference that is expected because of the known enthalpic stabilization of [65−72] (as discussed below). However, the slopes of the two individual trendlines for those bonds that could be paired with [65−72] and those that could not are 0.018 and 0.012, respectively (again excluding [65−72]), which is significantly greater than zero (the slope of all data points combined, shown in Figure 4, is 0.014). This suggests that the enhancement of relatively long disulfide loops is not due solely to the stability and length of 2S intermediates containing [65−72], because the trend shown in Figure 4 is, at least in part, not a function of the presence of [65−72].

A similar plot for the 1S intermediates based on the data of Xu et al. (*6*) shows an even stronger trend ($m = 0.026$, $R^2 = 0.446$, where R is the correlation coefficient). This trend cannot be even partially due to the stability of [65−72] as discussed above, since the 1S intermediates have only a single disulfide bond.

While quite good entropy predictions have been obtained using eqs 1 and 2 (*23*), they are not accurate enough for Figure 4 to be considered conclusive evidence for the compactness of the 1S and 2S intermediates. However, it lends support to the idea that the early disulfide intermediates in RNase A may be collapsed, in addition to being disordered.

Furthermore, it has been shown, by dynamic energy-transfer studies (*24*) and small-angle X-ray scattering (*25*), that *reduced* RNase A is at least partially compact. Additionally, dynamic light scattering measurements (*26)* indicate that reduced RNase A has a Stokes radius of 2.91 nm, intermediate between that of reduced-denatured RNase A, 3.14 nm, and disulfide-intact denatured RNase A, 2.60 nm. The compact state may arise because of hydrophobic interactions. This supports the above evidence, since a collapse of the reduced protein caused by hydrophobic interactions will also compact the structure of disulfide-containing intermediates.

Stability of Species with the Native Disulfide Bond [65−72]. The [65−72] bond is observed to make up 26.6% of the disulfide bonds in the 2S group, and accordingly, it is present in ∼53% of all 2S intermediates, as discussed above. Moreover, [65−72] lies significantly farther off of the trendline in Figure 4 than the noise distribution of the other bonds. This implies that [65−72] is specifically stabilized relative to the other intermediates. However, a more important factor implying its significance is the equilibrium constant K_{eq} between bonds [65−72] and [58−65], which

[5] More precisely, the slope is expected to be somewhat less than zero because of excluded volume effects, which will tend to expand the chain and therefore favor *small* loops over large loops. See, for example, ref *15*.

was determined from the ratio of their *experimental* percent abundances in Table 2 to be 4.5. This value of K_{eq} is significant in that its interpretation does not make use of the model on which eq 1 is based, because the two loops formed by these bonds have the same length (there is, however, a slight difference from unity for the predicted value of K_{eq}, 0.9, because of a positional effect with overlapping loops: bond [58−65] is able to form, on average, somewhat more stable overlapping loops with other disulfide bonds than [65−72], simply because of its position in the molecule[4]). Because of their identical loop size, the value of $K_{eq} = 4.5$ between these two species is strong evidence for energetic stabilization of [65−72] relative to [58−65].

The stability of bond [65−72] vs [58−65] has been demonstrated previously for a fragment of RNase A. Milburn and Scheraga found the equilibrium constant between the [65−72] and [58−65] isomers to be 5.9 ± 0.8 in the M peptide (residues 50−79) (*27*), while a synthetic peptide consisting of residues 58−72 was shown to favor bond [65−72] with a K_{eq} of 3.6 (*28*). Most interestingly, Xu et al. (*6*) also found a large K_{eq} of 4.2 in the 1S distribution.

What is stabilizing the [65−72] bond? Briefly, a type II β-turn was observed to form in residues 66−69 in the synthetic peptide 58−72 (*29*), and a type III β-turn was observed in residues 65−68 of the crystal structure of native RNase A (*30*, *31*) and in the NMR structure of the mutant (C40A, C95A) of RNase A (*32*). It can be inferred that this same local interaction probably stabilizes the disulfide bond [65−72] in the 1S and 2S species. The significance of these results for folding is discussed below.

The Role of the 2S Intermediates in RNase A Folding. It is important to understand the role that each group of disulfide-bonded intermediates (that are formed prior to the rate-determining step) plays in the folding mechanism of RNase A. These intermediates are in a preequilibrium during the steady-state period of folding (*8*) and, therefore, should be discussed in energetic, not kinetic terms (*33*). The rate-determining step consists of either a conformational change or thiol-disulfide exchange reaction in one or more key 3S intermediates (see Figure 1), here termed $3S_{precursor}$, to form either des-[65−72] or des-[40−95]. The rate of folding to native RNase A is determined by the concentration of $3S_{precursor}$ and the rate constant, which will be an apparent one if there are multiple precursors. Since the identities of the precursors are unknown, the available kinetic data are expressed in an apparent form in terms of all 3S intermediates, i.e.,

$$\frac{d[N]}{dt} = k_{apparent}[3S_{total}] = k_{precursor}[3S_{precursor}] \qquad (3)$$

Three implications regarding folding can be drawn from a knowledge of the nature of the 2S intermediates, as derived in this study, and from a knowledge of the 1S intermediates (*6*). First, although the 2S and 1S intermediates are not directly involved in the rate-determining step [except for *minor* pathways involving the oxidation of 2S to des-[40−95] and des-[65−72] (*4*, *5*)], they can modulate the folding rate through their stability relative to the precursor of the rate-limiting step. The more stable the 2S, 1S, and nonprecursor 3S intermediates relative to $3S_{precursor}$, the lower the concentration of the 3S precursors, making the folding rate slower. This follows from the simple kinetic scheme of eq 3.

Therefore, while it at first seems that the large number of globally disordered 2S intermediates may slow folding by acting as unproductive kinetic traps, their lack of stability may actually increase the rate of folding, by raising the concentrations of the kinetically important $3S_{precursor}$. This may be a general trend in protein folding. A good example of the opposite case is the folding of BPTI, in which an extremely stable intermediate lacking a single disulfide bond is unable to form the native state on a reasonable time scale (*34*).

Second, collapse of the 1S and 2S intermediates could lead to collapsed 3S intermediates. A collapsed state of the 3S intermediates (particularly in the $3S_{precursor}$) might increase the rate of folding by reducing the conformational space that the protein has to search to find its native state. While this collapse is not unlikely to occur considering the data reported here, no evidence is available regarding the nature of the 3S ensemble, to our knowledge.

Third, the dominance of the [65−72] bond provides clues about the nature of the 3S intermediates and their folding. Since the β-turn is a local, native structure, and is likely to be widely present in the 1S and 2S species (*27*−*29*), it is likely to be present in many of the 3S intermediates also. The β-turn could serve to increase the rate of folding by one or both of two mechanisms. (*i*) The $3S_{precursors}$ most likely have characteristics of nativelike structure, since these species are able to proceed directly to the native state at a reasonable rate. A nativelike β-turn could effectively increase the folding rate by raising the concentration of these $3S_{precursors}$, specifically, relative to other 3S species. In agreement with this, the folding intermediates of a mutant of RNase A with both the 65 and 72 cysteine residues replaced by serine or alanine were observed to be destabilized relative to wild-type RNase A (*5*). Additionally, this mutant protein was observed to fold at a rate which is significantly slower than the folding of wild-type RNase A. Since the β-turn is probably cooperatively stabilized by the [65−72] disulfide bond in wild type RNase, the mutant may have only a small amount, if any, of β-turn in the [65−72] loop region during folding. Furthermore, the native state of this same mutant ([C65S,C72S]) was found by NMR to lack the β-turn in the [65−72] loop region (*35*). (*ii*) This turn could also serve as a chain-folding initiation site (*8*, *36*) in the $3S_{precursor}$ which would accelerate further folding by decreasing the dimensionality of the conformational space which has to be searched. This reduction of the conformational space could act additively and perhaps even synergistically with the collapse-mediated (hydrophobic effect and/or disulfide-bond driven) reduction in conformational space. This is consistent with the three-disulfide species des-[40−95] (which contains [65−72]) being on the major folding pathway (80% of total flux) (*2*). The instability and high conformational entropy of des-[40−95] relative to des-[65−72] (*32*, *37*) may be a further reason why it lies on the major folding pathway; the transition state in the formation of des-[40−95] from $3S_{precursor}$ is likely to be stabilized by a relatively high entropy, resulting in an increased rate of folding through this pathway. Again, instability of folding intermediates counter-intuitively seems at times to play a role in *promoting* folding.

ACKNOWLEDGMENT

We thank Ervin Welker, Yue-Jin Li, Mahesh Narayan, and William Wedemeyer for insightful discussions.

REFERENCES

1. Rothwarf, D. M., Li, Y.-J., and Scheraga, H. A. (1998) *Biochemistry 37*, 3760.
2. Rothwarf, D. M., Li, Y.-J., and Scheraga, H. A. (1998) *Biochemistry 37*, 3767.
3. Li, Y.-J., Rothwarf, D. M., and Scheraga, H. A. (1998) *J. Am. Chem. Soc. 120*, 2668.
4. Xu, X., and Scheraga, H. A. (1998) *Biochemistry 37*, 7561.
5. Iwaoka, M., Juminaga, D., and Scheraga, H. A. (1998) *Biochemistry 37*, 4490.
6. Xu, X., Rothwarf, D. M., and Scheraga, H. A. (1996) *Biochemistry 35*, 6406.
7. Montelione, G. T., and Scheraga, H. A. (1989) *Acc. Chem. Res. 22*, 70.
8. Rothwarf, D. M., and Scheraga, H. A. (1993) *Biochemistry 32*, 2671.
9. Creighton, T. E. (1977) *J. Mol. Biol. 113*, 295.
10. Bruice, T. W., and Kenyon, G. L. (1982) *J. Protein Chem. 1*, 47.
11. Thannhauser, T. W., Konishi, Y., and Scheraga, H. A. (1984) *Anal. Biochem. 138*, 181.
12. Thannhauser, T. W., McWherter, C. A., and Scheraga H. A. (1985) *Anal. Biochem. 149*, 322.
13. Rothwarf, D. M., and Scheraga, H. A. (1993) *Biochemistry 32*, 2680.
14. Lin, S. H., Konishi, Y., Denton, M. E., and Scheraga, H. A. (1984) *Biochemistry 23*, 5504.
15. Flory, P. J. (1953) *Principles of Polymer Chemistry*, Chapter X, Cornell University Press, Ithaca, NY.
16. Poland, D. C., and Scheraga, H. A. (1965) *Biopolymers 3*, 379.
17. Weissman, J. S., and Kim, P. S. (1991) *Science 253*, 1386.
18. Konishi, Y., and Scheraga, H. A. (1980) *Biochemistry 19*, 1308.
19. Konishi, Y., and Scheraga, H. A. (1980) *Biochemistry 19*, 1316.
20. Creighton, T. E. (1979) *J. Mol. Biol. 129*, 411.
21. Staley, J. P., and Kim, P. S. (1992) *Proc. Natl. Acad. Sci. U.S.A. 89*, 1519.
22. van Mierlo, C. P. M., Darby, N. J., Keeler, J., Neuhaus, D., and Creighton, T. E. (1993) *J. Mol. Biol. 229*, 1125.
23. Pace, C. N., Grimsley, G. R., Thomson, J. A., and Barnett, B. J. (1988) *J. Biol. Chem. 263*, 11820.
24. Buckler, D. R., Haas, E., and Scheraga, H. A. (1995) *Biochemistry 34*, 15965.
25. Zhou, J.-M., Fan, Y. -X, Kihara, H., Kimura, K., and Amemiya, Y. (1998) *FEBS Lett. 430*, 275.
26. Nöppert, A., Gast, K., Müller-Frohne, M., Zirwer, D., and Damaschun, G. (1996) *FEBS Lett. 380*, 179.
27. Milburn, P. J., and Scheraga, H. A. (1988) *J. Prot. Chem. 7*, 377.
28. Altmann, K.-H., and Scheraga, H. A. (1990) *J. Am. Chem. Soc. 112*, 4926.
29. Talluri, S., Falcomer, C. M., and Scheraga, H. A. (1993) *J. Am. Chem. Soc. 115*, 3041.
30. Borkakoti, N., Moss, D. S., and Palmer, R. A. (1982) *Acta Crystallogr., Sect. B 38*, 2210.
31. Wlodawer, A., Svensson, L. A., Sjölin, L., and Gilliland, G. L. (1988) *Biochemistry 27*, 2705.
32. Laity, J. H., Lester, C. C., Shimotakahara, S., Zimmerman, D. E., Montelione, G. T., and Scheraga, H. A. (1997) *Biochemistry 36*, 12683.
33. Konishi, Y., Ooi, T., and Scheraga, H. A. (1982) *Biochemistry 21*, 4741.
34. Creighton, T. E., and Goldenberg, D. P. (1984) *J. Mol. Biol. 179*, 497.
35. Shimotakahara, S., Rios, C. B., Laity, J. H., Zimmerman, D. E., Scheraga, H. A., and Montelione, G. T. (1997) *Biochemistry 36*, 6915.
36. Matheson, R. R., Jr., and Scheraga, H. A. (1978) *Macromolecules 11*, 819.
37. Li, Y.-J., Rothwarf, D. M., and Scheraga, H. A. (1995) *Nat. Struct. Biol. 2*, 489.

BI990570F